

Stable Copper Nanoparticle Photocatalysts for Selective Epoxidation of Alkenes with Visible Light

Yiming Huang, Zhe Liu, Guoping Gao, Gang Xiao, Aijun Du, Steven E. Bottle, Sarina Sarina, and Huaiyong Zhu

ACS Catal., **Just Accepted Manuscript** • Publication Date (Web): 19 Jun 2017

Downloaded from <http://pubs.acs.org> on June 19, 2017

Just Accepted

“Just Accepted” manuscripts have been peer-reviewed and accepted for publication. They are posted online prior to technical editing, formatting for publication and author proofing. The American Chemical Society provides “Just Accepted” as a free service to the research community to expedite the dissemination of scientific material as soon as possible after acceptance. “Just Accepted” manuscripts appear in full in PDF format accompanied by an HTML abstract. “Just Accepted” manuscripts have been fully peer reviewed, but should not be considered the official version of record. They are accessible to all readers and citable by the Digital Object Identifier (DOI®). “Just Accepted” is an optional service offered to authors. Therefore, the “Just Accepted” Web site may not include all articles that will be published in the journal. After a manuscript is technically edited and formatted, it will be removed from the “Just Accepted” Web site and published as an ASAP article. Note that technical editing may introduce minor changes to the manuscript text and/or graphics which could affect content, and all legal disclaimers and ethical guidelines that apply to the journal pertain. ACS cannot be held responsible for errors or consequences arising from the use of information contained in these “Just Accepted” manuscripts.



Stable Copper Nanoparticle Photocatalysts for Selective Epoxidation of Alkenes with Visible Light

Yiming Huang,[†] Zhe Liu,[†] Guoping Gao,[†] Gang Xiao,[‡] Aijun Du,[†] Steven Bottle,[†] Sarina Sarina^{*,†} and Huaiyong Zhu^{*,†}

[†]School of Chemistry, Physics and Mechanical Engineering, Faculty of Science and Engineering, Queensland University of Technology, Brisbane, QLD 4001, Australia

[‡]Key Laboratory of Bioprocess, Beijing University of Chemical Technology, Beijing, 100029, P. R. China.

ABSTRACT: Selective epoxidation of various alkenes with molecular oxygen (O₂) under mild conditions is a long standing challenge in achieving syntheses of epoxides. Cu based catalysts have been found to be catalytically active for selective epoxidations. However the application of copper nanoparticles (CuNPs) for photocatalyzed epoxidations is encumbered by the instability of CuNPs in air. Herein we report that CuNPs supported on titanium nitride (TiN) without additional stabilizers, not only are stable in air, but also can catalyze selective epoxidation of various alkenes with O₂ or even air as benign oxidant under light irradiation. CuNPs remain in the metallic state due to the significant charge transfer that occurs between CuNPs and TiN. The epoxidation is driven by visible light irradiation at moderate temperatures, achieving good-to-high yields and excellent selectivity. The photocatalytic process is applicable to the selective epoxidation of various alkenes. In this photocatalytic system, reactant alkenes chemically adsorb on CuNPs forming Cu-alkene surface complexes and light irradiation can activate the complexes for reaction. The cyclic ether solvent also plays a key role, reacting with O₂ on the surface of CuNPs under light irradiation, yielding oxygen adatoms. The activated surface complexes react with the adatoms, yielding corresponding epoxides. Analysis of the influence of irradiation wavelength and intensity on the epoxidation suggests that light-excited electrons of CuNPs drive the reaction. The adatoms formed react with alkenes producing the final product epoxides. We also observed interesting product stereo-selectivity predominantly generating the *trans*-isomers for the epoxidation of stilbene (up to 97%). The findings reported here not only provide an effective and selective reaction system for alkene epoxidations, but also are a step towards demonstrating the practical use of CuNPs as photocatalysts for various applications.

Introduction

Selective epoxidation of alkenes is a reaction of great interest because epoxides are versatile building blocks in organic syntheses, the pharmaceutical industry and in materials and life sciences.¹⁻³ At the forefront of existing challenges is the development of processes that use a benign oxidant, have broad substrate scope while maintaining high selectivity, high atom economy and reduced environmental impact.⁴

The use of metal-based homogeneous catalysts has a rich history and has been comprehensively reviewed,⁵ however such catalysts can be costly and not eco-friendly.^{6,7} In the last decade, heterogeneous metal catalysts from group IB (Au, Ag, Cu etc.) have been found to be highly effective in epoxidations in the presence of activated oxygen atoms. It is generally accepted, although the exact details remain to be determined, that an oxametallacyclic (OME) intermediate is the key species in the catalytic cycle that drives the epoxidation.⁸⁻¹³

In the past decade, the direct utilization of solar energy over various forms of photocatalyst to promote organic synthesis has been recognized as perspective strategies.¹⁴⁻¹⁷ Among such, Au, Ag, Cu and Al, as plasmonic metals, their nanoparticles (NPs) exhibit remarkable visible light

adsorption due to the localized surface plasmon resonance (LSPR) effect.¹⁸⁻²² Free electrons of such NPs can also absorb ultraviolet, visible and infrared photons because these metals have continuous electron energy levels. Thus NPs of these metals can utilize light energy arising from most of the solar spectrum for catalysis.²³ The light irradiation generate photoexcited electrons and these electrons can transfer energy to molecules absorbed on the metal surface, inducing a range of chemical transformations.²⁴⁻³²

Consequently, the NPs of group IB metals represent excellent candidates for the development of new photocatalysts for epoxidations. Copper has the lowest cost among the IB metals, whereas it also exhibits the highest selectivity.¹³ Studies and applications of CuNPs are, however, strictly limited because CuNPs can be readily oxidized by air, oxidizing support materials and oxidants in the reaction environment, yet there is evidence that the metallic state of Cu is critical for both the optical properties of the catalyst and the epoxidation selectivity.³³ Polymer stabilizers and/or inert atmospheres have been employed to maintain copper in the metallic state.³⁴ Nitrobenzene reduction over a Cu@graphene photocatalyst has been reported,³⁵ in which CuNPs stay in the metallic

state on the graphene support. As yet there has been no in depth study to establish the basis of the stabilization effect. In this work, we demonstrate that CuNPs can be prevented from oxidation when titanium nitride (TiN) is used as a support, on which copper is dispersed as nanoparticles. Density function theory (DFT) calculations suggest that the significant charge transfer loop between CuNPs and TiN support provides the resistance of CuNPs towards oxidation.

Another challenge for selective epoxidation is using molecular oxygen as the oxidant for the epoxidation of alkenes at mild temperatures. Oxygen, especially if delivered in air, represents the ideal oxidant, superior even to the well-known “green” oxidant hydrogen peroxide.^{36,37}

In addition, low reaction temperatures are usually employed for photocatalysis processes, which not only reduce the energy consumed by the reaction, but also allow the process to be applied to temperature sensitive substrates. Despite these attractions, the use of O₂ as a selective oxidant and Cu-based catalysts under mild conditions has been faced with some challenges.^{38,39} In this study, we overcame many of these obstacles by using a novel copper supported photocatalyst (Cu@TiN) and a cyclic ether solvent, successfully achieving epoxidation of a range of alkenes with molecular oxygen under visible light irradiation at moderate reaction temperatures. Preliminary investigations of the photocatalytic epoxidation mechanism suggest a process involving adsorbed oxygen interacting with solvent to transfer oxygen atoms to the alkene.

Results and discussion

Metallic state of air-stable CuNPs. The photocatalyst is readily prepared by impregnation-reduction methodology to load CuNPs onto TiN powder (with particle size ~30 nm). In the as-prepared sample, copper exists at mixed oxidation states according to the XPS spectrum (shown in Figure S1a in Supporting Information, SI). This sample was labeled as CuO/Cu@TiN. The CuO/Cu@TiN was further treated under a hydrogen atmosphere at 300°C to secure the NPs in metallic state (Cu@TiN), this is confirmed by the XPS result shown in Figure 1). The binding energies at around 952.0 eV and 932.5 eV are indicative of the existence of Cu(0), and peaks for other oxidation states are notably absent.

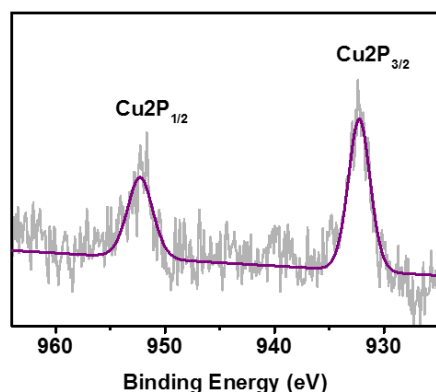


Figure 1. XPS spectrum of Cu@TiN photocatalyst suggests the metallic state of air-stable CuNPs. Air-stable metallic CuNPs supported by TiN substrate.

Transmission electron microscopy (TEM) images indicate that well-dispersed CuNPs (with a mean size of 4 nm) are distributed on the TiN surface (Figure 2a). Scanning electron microscopy (SEM) images and energy dispersive spectrometer (EDX) mapping shown in Figure S3 confirm the elemental composition of Cu@TiN is as designed. A representative single-crystal Cu NP with (111) lattice planes predominantly exposed is illustrated in Figure 2b. It has previously been reported that the (111) planes of Cu are favored for the absorption of reactants such as styrene.⁴⁰ O₂ can also be absorbed easily onto the surface of the (111) plane and this likely to represent the first step of oxygen activation.¹³ XRD patterns indicate that CuNPs have negligible impact on the TiN crystal structure presumably due to the low copper loading (Figure 2c).

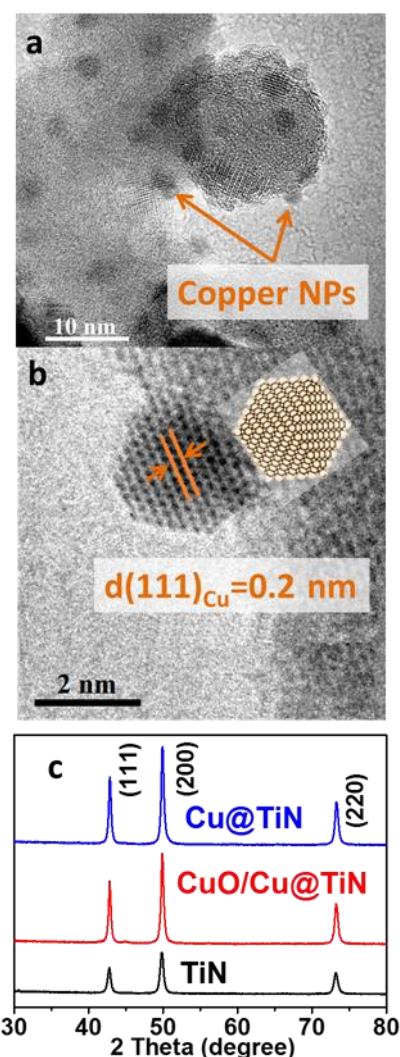


Figure 2. TEM and XRD characterizations of Cu@TiN. (a) TEM image of Cu@TiN, CuNPs are well dispersed on TiN substrate. (b) High resolution TEM image, single crystal CuNP was form on the surface of TiN substrate with clear (111) index face. (c) XRD patterns of the Cu@TiN, CuO/Cu@TiN and TiN. Cu@TiN exhibits identical XRD

peaks compared with TiN substrate indicating negligible influence of CuNPs loading on the TiN substrate.

The light absorption of TiN and Cu@TiN were examined by diffuse reflectance UV-Vis (DR-UV/Vis) spectra (Figure 3). Distinctly different light absorption in visible range is observed between TiN and Cu@TiN material. We further analyzed the UV-Vis spectrum of Cu@TiN by using TiN spectrum as background and obtained a spectrum attributed to isolated CuNPs as shown in the insert in Figure 3. This indicates that CuNPs exhibit strong visible light absorption with peak at around 580 nm being the characteristic LSPR absorption of CuNPs.^{35,41}

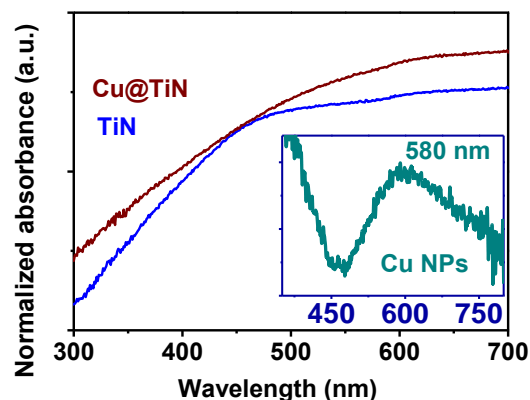


Figure 3. DR-UV-Vis spectra of Cu@TiN, TiN and isolated CuNPs (insert); Cu loading has a significant impact on the optical properties of the TiN substrate; the isolated spectrum of CuNPs was obtained by measuring Cu@TiN using TiN as background, peak at 580 nm is attributed to the LSPR peak of CuNPs.

To provide an in-depth understanding of the stabilization mechanism for CuNPs supported on the TiN substrate, we have carried out systematic DFT calculations for the Cu/TiN interface. Figure 4 presented a side view of 3D plot of charge density difference for CuNPs on the TiN surface. Yellow and cyan iso-surfaces represented charge accumulation and depletion in the 3D space with an iso-surface value of $0.005 \text{ e}/\text{\AA}^3$.

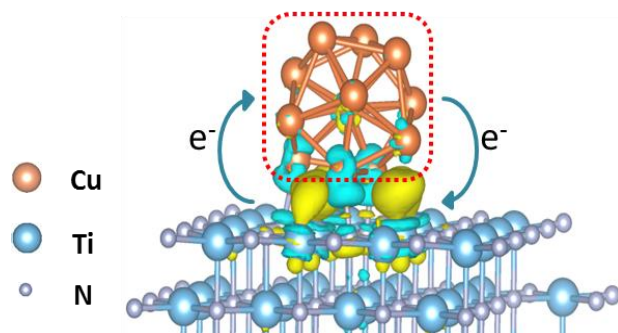


Figure 4. Structure and charge density difference plot at the CuNPs/TiN interface simulated using DFT method. Charges are transferred from Cu atoms to N atoms, and a similar degree of charge transfer from Ti atoms back to Cu results in

the stabilization of CuNPs on the TiN substrate. The oxidation state of Cu@TiN was calculated to be $+0.02$.

Clearly, there is a significant charge transfer from the CuNPs to the N atoms of the TiN substrate, which can be the major reason for CuNPs being more stable. Importantly, an equal amount of charge is donated back from the Ti atoms of TiN to the CuNPs. Such a charge exchange between the CuNPs and the TiN support consequently gives rise to a slightly positively charged state ($+0.02$) for the CuNPs, thus suggesting a negligible oxidation state of Cu atom. The stabilization of CuNPs is also confirmed by the large negative formation energy (-4.08 eV) of Cu@TiN.

Photocatalytic performance of Cu@TiN for epoxidation of alkenes. We found that the new Cu@TiN photocatalyst exhibits excellent activity for selective epoxidation of various alkenes using air or molecular oxygen as the oxidant under visible light irradiation at 60°C . Table 1 shows the results of the representative epoxidation of styrene, *trans*-stilbene and norbornene (Table 1, entries 1, 4 and 5). The photocatalytic epoxidation using air as oxidant proceeds smoothly over the Cu@TiN photocatalysts under moderate/mild reaction conditions. The significant difference in both conversion and selectivity between light irradiated reactions and the same reactions in the dark (numbers in parentheses) confirms that light absorption is the major driving force for the reactions.

We also observed only a certain degree of photocatalytic-performance from the TiN support material alone (Table S1). The TiN support exhibits light adsorption (Figure 3) and results in 40% conversion for oxidizing styrene to benzaldehyde yet no epoxides product was detected, which is a critical issue in the epoxidation of terminal alkenes. In the contrast, with CuNPs loaded TiN photocatalyst, we observed 100% conversion with 89% selectivity towards epoxides product, demonstrating the support makes little contribution to the overall conversion and selectivity of the Cu@TiN catalyst.

The epoxidation over Cu@TiN is inhibited when air or pure O_2 is replaced by argon (Table 1, entry 3; Table S2) indicating that molecular oxygen is required as the oxidant in the process. It also reveals the fact that Cu@TiN can cooperate with O_2 while maintaining its metallic state.

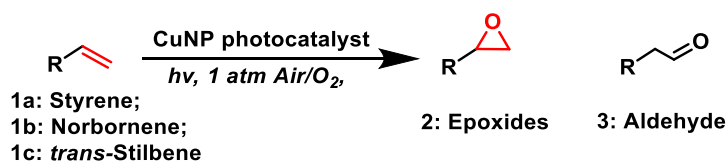
The important role of the metallic state CuNPs in the epoxidation is also demonstrated in Table 1. The precursor powder CuO/Cu@TiN comprises both metallic and oxidized Cu, as confirmed by XPS measurements (Figure S1a). We applied CuO/Cu@TiN in photocatalytic epoxidations as well as CuO@ZrO₂ (XPS spectrum in Figure S1b), commercial Cu oxides and salts for comparison. It should be noted that Cu oxides are *p*-type semiconductors with narrow band gaps and can also absorb visible light (see the reflectance UV-Vis extinction spectra in Figure S2a).⁴² Thus, as expected, we observed some light induced conversion with CuO/Cu@TiN, CuO@ZrO₂ and commercial CuO and Cu₂O powder (with much higher Cu content); although none of these materials proved as effective as

metallic Cu@TiN (Table 1, entries 6-11). It has been previously reported that copper salts, complexes or oxides exhibit catalytic activity for epoxidation of alkenes in the assistance of stronger oxidants than molecular oxygen.^{43,44}

This may explain the very low conversion that we observed with copper oxide catalyst using molecular oxygen

Table 1. High performance epoxidation of alkenes over Cu@TiN.^[a]

in the dark. Thus, on the basis of the results in Table 1, we conclude that metallic state CuNP plays an important role in the activation of molecular oxygen, whereas copper oxides are much less effective.



Entry	Catalyst	Atmosphere	Substrate	Conv. [%]	Select. [%]	
					2	3
1	Cu@TiN	Air ^[b]	1a	100(6)	89(n.d)	11(100)
2	Cu@TiN	O ₂	1a	100(5)	81(n.d)	19(100)
3	Cu@TiN	Argon	1a	n.r.	n.d.	n.d.
4 ^[c]	Cu@TiN	Air ^[b]	1b	100(14)	100(100)	n.d(n.d)
5 ^[d]	Cu@TiN	Air ^[b]	1c	100(23)	100(100)	n.d(n.d)
6	CuO/Cu@TiN	O ₂	1a	85(13)	44(19)	56(81)
7 ^[c]	CuO/Cu@TiN	O ₂	1b	36(4)	100(100)	n.d(n.d)
8 ^[d]	CuO/Cu@TiN	O ₂	1c	72(20)	100(100)	n.d(n.d)
9	CuO@ZrO ₂	O ₂	1a	74(25)	32(20)	68(80)
10	CuO ^[e]	O ₂	1a	87(7)	53(n.d)	47(100)
11	Cu ₂ O ^[e]	O ₂	1a	79(4)	54(n.d)	46(100)
12	Cu(NO ₃) ₂ ^[e]	O ₂	1a	7(3)	n.d(n.d)	100(100)
13	None	O ₂	1a	6	n.d	100

Reaction conditions: 20 mg catalyst, 0.1 mmol substrate and 3 mL 1,4-dioxane as solvent. Selected gas was bubbled for 5 min and then reaction tube was sealed. The reaction mixture was stirred under visible light irradiation (0.5 W/cm²) at 60°C for 4 h. Conversion were determined by using an Agilent 6980 gas chromatography coupling with an Agilent HP5973 mass spectrometer equipped with a HP-5 column (GCMS). Numbers in parentheses are results of reactions in the dark. [a] (n.r.= no reaction; n.d.=not detected); [b] air was bubbled for 5 min prior to the start of reaction and every hour after; [c] reaction for 8 h; [d] reaction for 16 h; [e] the Cu loading of the catalyst is 40 times of that in Cu@TiN.

More importantly, in the epoxidation of terminal alkenes, where aldehyde can be easily formed as by-product, the work of Marimuthu *et al* had proved that metallic state CuNPs are superior to copper oxides in respect to epoxidation selectivity,³³ a possible reason is the direct electron photoexcitation between hybridized orbitals of metal-organic as such effect does not occur on copper oxides (comparing the results of entries 2, 6 and 9 in Table 1), this theory will be further discussed later. Cu(NO₃)₂ showed negligible activity in both light irradiated and dark reactions (Table 1, entry 12) demonstrating the ineffectiveness of Cu²⁺ ions in epoxidation of alkenes. The blank reaction of styrene epoxidation was also tested in the absence of any catalyst showing a 6% conversion with only benzaldehyde product as shown in (Table 1, entry 13).

As shown in Table 2, Cu@TiN photocatalyst exhibits wide substrate scope while maintaining excellent selectivity, being active on linear, aromatic, terminal, electron

deficient, electron rich and conjugated alkenes. For example, good to excellent yields were achieved for epoxidation of terminal alkenes. This is of particular interest as the 1,2-epoxide products are often key intermediates in organic synthesis (Table 2, entries 1, 2, 4 and 5 etc.).⁴⁵⁻⁴⁷ Epoxidation of electron-deficient alkenes, which is regarded to require strong oxidants,⁵ was achieved with excellent selectivity using Cu@TiN (Table 2, entries 7 and 8).

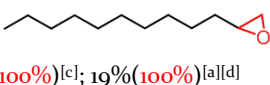
It has been reported that terminal alkenes are less active in epoxidation reactions than cyclo-alkenes,⁴⁸ because low electron density of terminal alkenes has negative impact on the electrophilic oxygen transfer and results in reduced reactivity.⁴⁹ In the present study, poor conversion is observed for cyclohexene and its derivative (Table 2, entries 9 and 10), while the reaction of 1-hexene achieved good yield (Table 2, entry 20).

We also found that increasing the strain energy of cycloalkanes can remarkably promote the reaction efficiency. Two examples, cyclooctene and norbornene are shown in Table 2 (entries 11 and 12). Nonetheless, low selectivity for the epoxide product is observed for propene epoxidation over Cu@TiN although the propene conversion is high. The predominant product in this case is the ketone (Table 2, entry 13) rather than the epoxide, the reason has not been understood yet.

Cu@TiN photocatalyst also exhibited very good performance for reactants with terminal conjugated double

bonds (Table 2, entries 14-16) due to the strong adsorption of π -conjugated molecules on to the Cu surface. Such adsorption lowers the LUMO energy of the adsorbate.⁵⁰ Poor yields are observed with relatively inactivate aliphatic long-chain alkenes (Table 2, entries 18 and 19). Nevertheless, employing a stronger oxidant such as H₂O₂ can effectively enhance the reaction efficiency (see entries 18 and 19 under conditions d), indicating the Cu@TiN can interact with other oxidants to transform less reactive alkenes to the corresponding epoxides.

Table 2. Scope of the Cu@TiN catalyzed epoxidation reaction of alkenes. The performance is expressed in conversion of the reactant and selectivity to the corresponding epoxide product (percentage in parentheses)

[1] 	[2] 	[3] 	[4] 
72%(83%)	100%(78%)	100%(100%)	100%(53%)
[5] 	[6] 	[7] 	[8] 
25%(63%)	3%(100%) ^[b]	100%(100%)	45%(100%) ^[a]
[9] 	[10] 	[11] 	[12] 
15%(100%) ^[a]	7%(100%) ^[a]	50%(100%) ^[a]	100%(100%) ^[b]
[13] 	[14] 	[15] 	[16] 
100%(5%) ^[b]	85%(100%) ^[b]	100%(65%) ^[b]	100%(100%)
[17] 	[18] 	[19] 	
100%(15%)	32%(100%) ^[c] 65%(100%) ^{[a][d]}	14%(100%) ^[c] ; 19%(100%) ^{[a][d]}	
[20] 	[21] 	[22] 	[23] 
83%(100%) ^[a]	55%(100%) ^[a]	32%(100%) ^[a]	71%(100%) ^[a]
[24] 	[25] 	[26] 	
59%(100%) ^[a]	100%(89%) ^[a]	28%(100%) ^[a]	

Reaction conditions: 20 mg Cu@TiN, 0.1 mmol reactant and 3 mL solvent. O₂ was bubbled for 5 min. and then the reaction tube was sealed. The reaction mixture was stirred under visible light irradiation (0.5 W/cm²) at 60°C for 4 h [a] reaction time 16 h; [b] reaction temperature 40°C, reaction time 8 h; [c] reaction temperature 70°C, reaction time 48 h; [d] 2 equiv. H₂O₂ (0.2 mmol) was added as oxidant. Conversion (dark color numbers) and selectivity (red color numbers) were determined by GCMS analysis. For entries 21-26, starting reactants are *trans*-2-hexene, *cis*-2-hexene, *trans*-3-hexene, *cis*-3-hexene, *trans*-stilbene and *cis*-stilbene, for possible enantiomer products, only one enantiomer is presented.

It is noteworthy that the photocatalytic epoxidation system favors *trans*-epoxide over their *cis*-isomers (Table 2, entries 21-26). This stereo-selectivity is evident as the

results in Table 3 show that the *trans*-epoxide is predominant product no matter *cis*- or *trans*-stilbene were used

as reactant. Conversion of the *cis*-stilbene is substantially lower than that *trans*-stilbene.

It is known that both photo induced isomerizations from *cis*-stilbene to *trans*-stilbene and from *trans*-stilbene to *cis*-stilbene can take place.⁵¹ But there is a larger barrier (~3 kcal/mol) for the *trans*- to *cis*-isomerization than for the reverse reaction (the barrier is negligible). *Trans*-stilbene should be less reactive than *cis*-stilbene from the point of view of energy. In the contrary, results in Table 3 are against the inference. This indicates the stereo-selectivity over Cu@TiN photocatalyst is not determined solely by bond energy. Importantly, under the photocatalytic conditions of the present study, we did not observe direct *trans*- to *cis*- isomerization of alkene reactants in experiments. Therefore, we deduce that the stereo-selectivity is integrated into the epoxidation process. Similar results have been reported with Au/C catalyst, it was believed that the adsorption of olefins onto metal surface may create steric constraints, resulting in a specific reaction pathway.⁵² Another possible explanation is that the isomerization on CuNP surface is caused by light irradiation.⁵³

Table 3. Stereo-selectivity of stilbene epoxidation

Entry	Substrate	Light	Conversion %	Selectivity %
1	<i>trans</i> - Stilbene	Light	100	89 (<i>trans</i>)
		Dark	12	98 (<i>trans</i>)
2	<i>cis</i> - Stilbene	Light	28	95 (<i>trans</i>)
		Dark	n.r.	n.d.
3 ^[a]	<i>mixed</i> - Stilbene	Light	76	97 (<i>trans</i>)
		Dark	5	99 (<i>trans</i>)

Reaction conditions: 20 mg Cu@TiN, 0.1 mmol substrate, 3 ml 1,4 dioxane as solvent, O₂ bubbled for 5 min, 60°C, 0.5 W/cm², 16 h. [a] mixed stilbene was prepared by mixing *trans*-stilbene and *cis*-stilbene in 1:1 ratio. (n.r. = no reaction; n.d. =not detected)

Catalytic active sites of Cu@TiN. To study the active sites, we measured infrared emission spectra (IES) of styrene adsorbed on Cu@TiN photocatalyst and TiN support, respectively, at stepwise elevated temperatures. As shown in Figure 5, the characteristic peaks of aromatic C=C stretch located at around 1400 cm⁻¹ can be identified for styrene adsorbed on both Cu@TiN and TiN at 50°C. It confirms the existence of styrene on Cu@TiN photocatalyst and TiN support material. These peaks can still be observed from the spectra of styrene adsorbed on Cu@TiN when the sample was heated to 450°C, as shown in Figure 5a, suggesting a strong chemisorption of styrene on the sample. In contrast, as shown in Figure 5b, the characteristic aromatic C=C peaks from the sample of styrene adsorbed on TiN are greatly weakened with raised temperature and nearly vanished at 300°C.

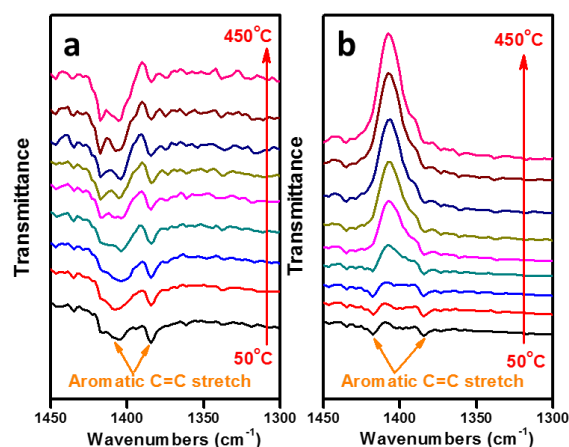


Figure 5. Infrared emission spectra of styrene adsorbed on (a) Cu@TiN photocatalyst and (b) TiN support. The infrared spectra were measured from 50°C to 450°C at every 50°C gap.

The results reveal that chemisorption of styrene on CuNPs is much stronger than that on TiN metal. Thus, it is rational that CuNPs, rather than TiN support, are the active sites. It was reported that chemisorption of styrene on Cu surface of (111) plane lowered unoccupied molecular orbitals (LUMOs) and elevated occupied molecular orbitals (HOMOs).⁴⁰ This is caused by the hybridization of Cu *d*-band orbitals and styrene π_1^* and π_2^* orbitals into bonding and antibonding orbitals of Cu-styrene surface complexes. Electrons from such complexes can be directly photo-excited between bonding and antibonding states, similar to the situation reported by Christopher *et al.*⁵⁴ Such excitation activates the double bond for epoxidation, enhancing photocatalysis activity and well-controlled selectivity (Table 1, entry 1). This theory can explain the fact that Cu@TiN exhibits photocatalytic performance superior to CuO/Cu@TiN and other Cu(I) and Cu(II) photocatalysts.

Influence of light. The effect of light on the reaction was examined to provide insights into the photocatalysis mechanism. Firstly, the irradiation wavelength has a crucial impact on the photocatalytic epoxidation can be directly reflected by action spectrum analysis, which shows a variation of the photocatalytic activity (in quantum yield) as a function of the irradiation wavelength.⁵⁵ We found that the trend of quantum yields (orange dots in Figure 6) does not follow the trend of light absorption shown by the DR-UV/Vis spectrum of Cu@TiN (the dash lines in Figure 6). However, in the wavelength ranging from 365 nm to 490 nm, the trend of the action spectra of all the reaction match well to the light absorption spectrum of isolated CuNPs (solid blue lines in Figure 6). The matching for *cis*-stilbene even extends to 530 nm. These results further demonstrate that CuNPs are the photocatalytic sites and TiN surface sites have very limited contribution to the photocatalytic epoxidation. This is consistent with reactant adsorption results obtained by IES

spectroscopy. In this wavelength range, stronger absorption by CuNPs results in a higher quantum efficiency.

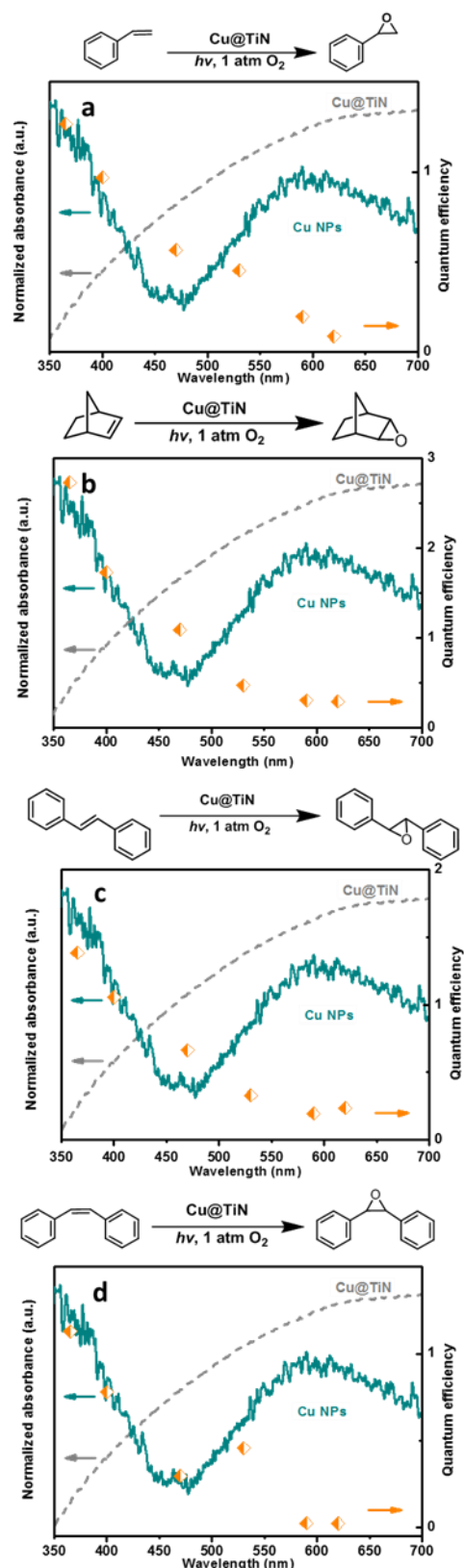


Figure 6. Action spectrum of (a) styrene, (b) norbornene, (c) *trans*-stilbene and (d) *cis*-stilbene epoxidation. Reaction

rates presented as quantum efficiency are plotted against wavelength of irradiated light at 400 ± 5 nm, 470 ± 5 nm, 530 ± 5 nm, 590 ± 5 nm and 620 ± 5 nm, 0.2 W/cm².

Nonetheless, the CuNPs can strongly absorb light in the range from 530 nm to 630 nm according to the DR-UV-Vis spectrum of isolated CuNPs, the quantum efficiency of Cu@TiN in this range is rather low and does not follow the trend of the LSPR adsorption of CuNPs. This fact clarifies two key issues.

First, the dependence on wavelength indicates that the contribution from the photo-thermal effect to the reaction rate is not important. Absorption of light by the NPs may cause a short term temperature increase of the NPs, leading to the so-called photo-thermal effect.³² The elevated temperature on NP surface could enhance the catalytic reaction on particle surface, such temperature rising is stronger with longer light wavelength. However, the light source with wavelength >530 cannot drive the epoxidation efficiently even with relatively high light adsorption at such range. For example, CuNPs exhibit strong absorption at 580 nm but give a very low catalytic activity under irradiation at this wavelength. On the other hand, reaction with 400 nm light source, which is weak in photo-thermal effect, exhibits much higher reaction rate. Thus we conclude that the epoxidation was not driven by the photo-thermal effect but the direct photon energy.

Second, the steep drop of the catalytic performance under wavelengths >530 nm implies that there is a threshold of photon energy required for the reaction. In Figure 6a,b and c, the photons of long wavelengths (e.g. >570 nm) do not have sufficient energy to induce the epoxidation; therefore negligible quantum yield was observed even though significant light absorption occurs.⁵⁶ However, in Figure 6d, we observed a higher quantum yield for *cis*-stilbene epoxidation at wavelength 530 nm than that at wavelength of 470 nm, a possible explanation is that the energy threshold for *cis*-stilbene is relatively low that photons of 530 nm is sufficient to trigger epoxidation, as a result, the high light adsorption at such wavelength emerge to dominate the photocatalysis and leads to a quantum yield bounce.

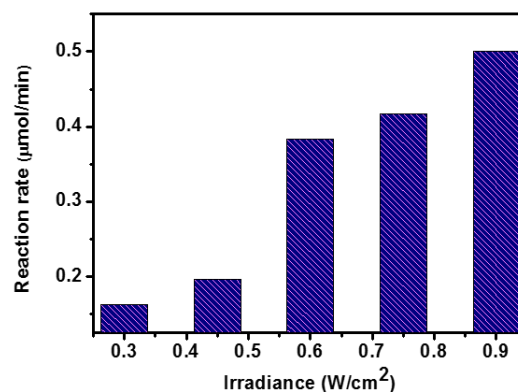


Figure 7. Dependence of photocatalytic activity on the light irradiance. 20 mg Cu@TiN, 0.1 mmol styrene and 3 mL 1,4-dioxane as solvent. Oxygen gas was bubbled for 5 mins and

then reaction tube was sealed. The reaction mixture was stirred under visible light irradiation (400-700 nm) at 60°C for 4 h. Conversion and selectivity were determined by GCMS analysis using HP-5 column. The reaction rate superlinearly increases with the increasing of light irradiance. [a] reaction time 3 h.

The relationship between photocatalytic performance and light irradiance (that is, the photon flux) was investigated through the epoxidation of styrene. Since the photons absorbed by the CuNPs induce the reactions, the light absorption should be proportional to the reaction yield. We observed a superlinearly increased photocatalytic activity with the increasing light irradiance as shown in Figure 7 and Table S3, this is proved to be one of the experimental signatures of photo-excited electron-driven reactions.⁵⁷ In general, high irradiance gives greater conversion and product yield, presumably through the more photoexcitation of the CuNPs. Additionally, more than one photoexcited electron may deposit their energies in one adsorbed reactant molecule at high light irradiance causing a superlinear reaction rate increase, which is a subsequent photoexcited electron deposits its energy in the reactant molecular before the dissipation of molecular vibration induced by another photo-excited electron.

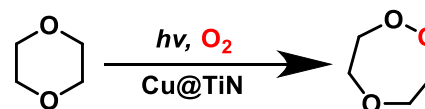
Influence of reaction temperature. We also investigated the influence of reaction temperature on the photocatalysis process. The temperature was adjusted by external heating or cooling. It was found that a moderate rise of reaction temperature can efficiently accelerate photocatalytic epoxidation of styrene (see Table S4). High reaction temperatures enhance the vibrational state of adsorbed reactant molecules,⁵⁷ so that less energy is required from photoexcited electron to overcome activation barrier. As a result, the Cu@TiN photocatalyst can utilize thermal energy to promote photocatalytic epoxidation as well, which is an advantage to traditional semiconductor photocatalysts.

Influence of solvent. To investigate the role of solvent for the epoxidation over Cu@TiN, we tested multiple organic solvents listed in Table S5. First of all, the most common solvents such as toluene, CH₂Cl₂, DMF and MeCN all give negative results, the results also illustrate that solvent polarity does not exhibit notable influence to the epoxidation. Moreover, high oxygen solubility is not crucial for epoxidation as we do not observe notable conversion with acetone and DMF. The determining factor of solvent was found to be the ether structure because we notice epoxidation over Cu@TiN only takes place in the presence of ether solvents, 1,4-dioxane, THF and diphenyl methyl ether for instance (Table S5). Therefore, we conclude that ethers structure, cyclic ethers in particular, play a key role in the reaction mechanism and the oxygen activation process as discussed in the subsequent section.

Mechanism study. The epoxidation mechanism of the new photocatalytic system must involve two general stages: 1) activation of molecular oxygen on CuNP surface; 2) selective epoxidation of C=C bond. Previous work in this area has shown that oxygen adatoms (O_a) adsorbed on CuNP, also referred as Cu-O species in many cases, have

been identified, both theoretically and experimentally, as the epoxidizing agent for alkene epoxidation.⁵⁸ Adsorption of O₂ on low index faces of Cu is facile,^{59,60} yet it is difficult to convert the adsorbed O₂ to O_a adatoms weakly bonded onto Cu surface. This is supported by the fact that Cu@TiN cannot initiate epoxidation in various solvents even those having high solubility of oxygen molecules (Table S5, entries 1-5). Successful epoxidations were only observed with 1,4-dioxane and other ethers, implying ether solvents played a crucial role in formation of O_a adatoms (Table S5, entries 6-10).

Table 4. The formation of peroxide intermediate.



Entry	Catalyst	Light	Atmosphere	Peroxide intermediate
1	Cu@TiN	Light	Oxygen	Detected
2	Cu@TiN	Light	Argon	Not detected
3	Cu@TiN	Dark	Oxygen	Not detected
4	No catalyst	Light	Oxygen	Not detected

Reaction conditions: 20 mg of 3 wt% Cu@TiN, 3 ml 1,4-dioxane as solvent, 60°C, light irradiance 0.5 W/cm², selected gas bubbled for 5 min, reaction time 2 h.

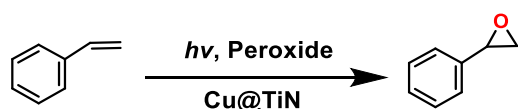
Taking 1,4-dioxane as an example (Table 4), GCMS analysis suggests that a seven-membered cyclic peroxide is produced from 1,4-dioxane. We found that the cyclic peroxide was produced within 2 h, only in the presence of both Cu@TiN catalyst and light irradiation as shown in Table 4. It means that 1,4-dioxane interacts with the adsorbed O₂ molecules on CuNP surface yielding the peroxide, and this process is predominantly driven by light irradiation due to the significant difference between light reaction and dark reaction.

We separated the liquid phase and solid catalyst of the system of entry 1 in Table 4, they are labeled as 1,4-dioxane-peroxide (the liquid) and Cu@TiN-peroxide (the solid), respectively. Both of them contain the seven-membered cyclic peroxide. Then we studied the function of the both, separately and in combination for styrene epoxidation reaction. The results are shown in Table 5.

Combining Cu@TiN-peroxide with 1,4-dioxane-peroxide exhibited similar yields (Table 5, entry 2) to that of a typical reaction without the peroxide (Table 5, entry 1). When oxygen was removed from reaction system, the typical reaction did not proceed (Table 5, entry 3). However, 8% yield was observed with the combined system (Table 5, entry 4). This is the evidence that the seven-membered cyclic peroxide provides the oxygen for epoxidation. We also found that epoxidation can proceed with Cu@TiN-peroxide alone (Table 5, entries 5 and 6) without oxygen source (neither oxygen gas nor ether), but cannot with 1,4-dioxane-peroxide alone (Table 5, entry 7). This

means that 1,4-dioxane-peroxide does not react directly with the C=C bond of styrene. Instead, there is an intermediate formed on the CuNPs, which is the direct cause of epoxidation reaction. This intermediate is generated from the reaction between from the seven-membered cyclic peroxide and the CuNP surface. Therefore, it is rational that the peroxide on CuNPs decompose to oxygen adatom (O_a) and 1,4-dioxane, the released oxygen adatoms act as oxidant which directly react with the C=C bond of alkene (which is activated by the photoexcitation of bonding electrons as afore discussed) as schematically illustrated in Scheme 1. The releasing of O_a does not require light irradiation, therefore we infer that light does not play critical rule in this step.

Table 5. Roles of 1,4-dioxane-peroxide and Cu@TiN-peroxide in epoxidation reaction.



Entry	Photocatalyst	Solvent	Atmosphere	Yield %
1	Cu@TiN	1,4-dioxane	Oxygen	53
2	Cu@TiN-peroxide	1,4-dioxane-peroxide	Oxygen	56
3	Cu@TiN	1,4-dioxane	Argon	0
4	Cu@TiN-peroxide	1,4-dioxane-peroxide	Argon	8
5	Cu@TiN-peroxide	Toluene	Argon	4
6	Cu@TiN-peroxide	1,4-dioxane	Argon	6
7	None	1,4-dioxane-peroxide	Argon	0
8	Cu@TiN	Toluene	Argon	0

Reaction conditions: 20 mg of photocatalyst, 3 ml solvent, 60°C, light irradiance 0.5 W/cm², selected gas bubbled for 5 min, reaction time 2 h.

It has been reported that styrene lays on a CuNP with C=C bond parallel to surface,^{12,13} and O_a reacts with the activated C=C bond causing the insertion of an O atom and producing the -C-C-O- structure. With such configura-

tion, two types of surface intermediates could be yielded according to previous studies on epoxidation.¹¹ One is a four-member oxametallacycle (OME-4) which includes one Cu atom bonded to both C and O atoms (see Scheme 1). The other is a five-membered OME (OME-5) involving a Cu-Cu fragment bonded to C and O atoms. The intermediate OME-5 would be expected to undergo a ring-opening process leading to undesired combustion products, while the -C-C-O- structure in OME-4 yields epoxide through a ring-closure process.¹¹ Thus, selectivity of epoxidation is determined in this step that occurs with lower activation energy. The overall reaction mechanism is shown in Scheme 1.

Interestingly, the selectivity also depends on the wavelength (Figure S4). When styrene is epoxidized with irradiation at 470 nm, we observed the highest selectivity, either shorter or longer wavelength light results in decreased selectivity towards epoxides. Photons with short wavelengths (<470 nm) are likely to lead to breakdown of the oxirane ring. This was confirmed experimentally through irradiation of styrene oxide that was shown to be unstable using shorter wavelength irradiation. On the other hand, photons with long wavelengths cannot deliver sufficient energy to trigger the epoxidation process resulting decreased selectivity as well as low conversions.

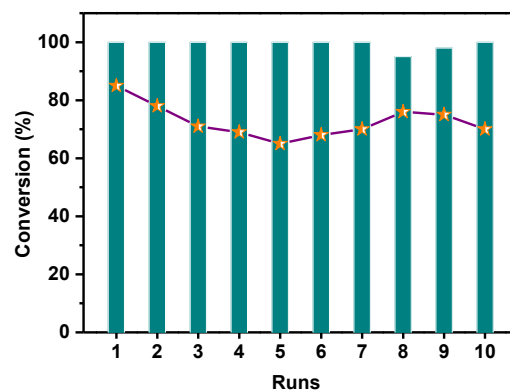
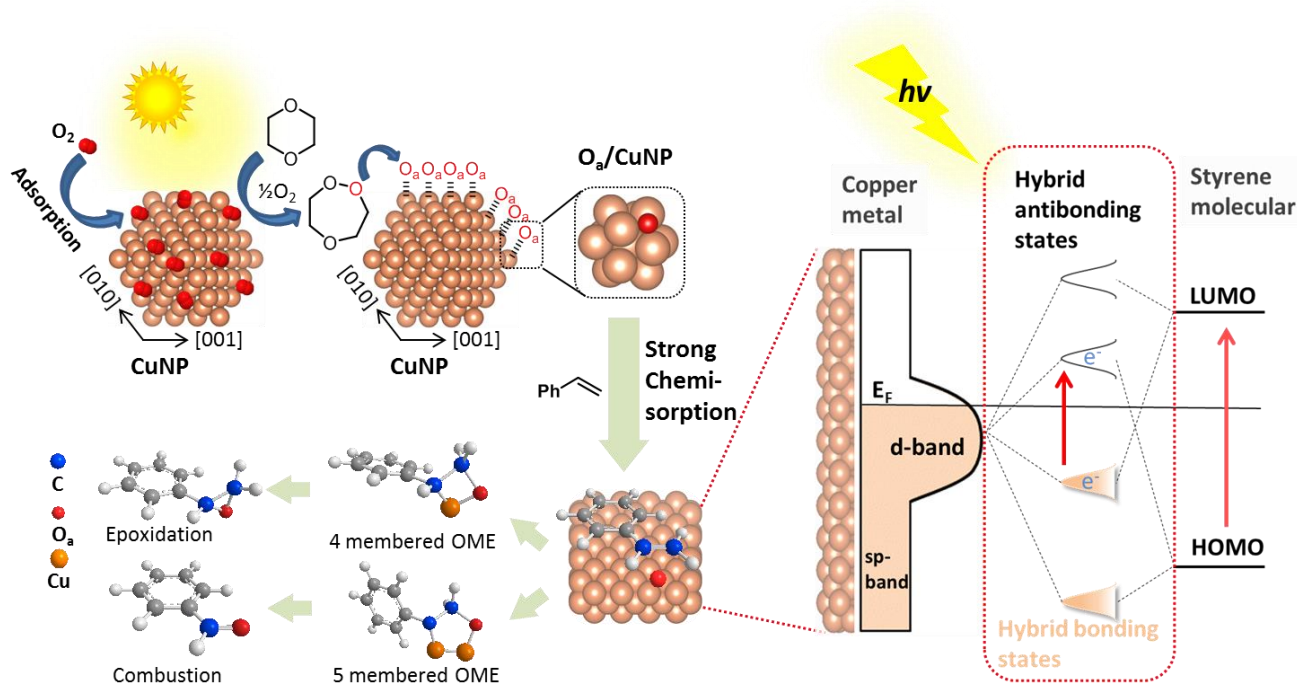


Figure 8. The reusability of the Cu@TiN. Epoxidation of styrene was used as module, used Cu@TiN photocatalyst was recovered, washed with water and ethanol and then directly applied in cycle reactions without further treatment or regeneration in the first seven cycle runs. Prior to the eighth cycle run, the used Cu@TiN photocatalyst was reactivated by hydrogen gas at 200°C for 10 mins. The bar chart represents the reaction conversion and the dot line represents the selectivity towards epoxides.

Scheme 1. Overall reaction mechanism of styrene epoxidation over Cu@TiN.



Oxygen molecules adsorb onto CuNPs first, and the consequent O_2 activation process occurs on the surface of CuNPs in the assistance of cyclic ethers under visible light irradiation at mild temperature ($<60^\circ\text{C}$). The adsorbed O_2 and cyclic ether yield cyclic peroxide, which then release oxygen adatoms (O_a) on the CuNP and the ether. Styrene strongly chemisorbs on the CuNPs surface forming Cu-styrene surface complex, and the chemisorption results in hybridization of Cu and styrene orbitals and formation of bonding and antibonding states. Hence, the light irradiation could induce direct resonant photoexcitation of electrons from hybrid bonding state to antibonding state to trigger the interaction between styrene and O_a adatoms. The oxidation of styrene on CuNP surface undergoes two competing reaction pathways through two types of OME intermediates and eventually give epoxidation product and combustion product respectively. E_F denotes the system Fermi level.

Reusability study. We also investigated the reusability of the Cu@TiN catalyst. The used photocatalyst was recovered, washed simply with water and ethanol and then directly applied in cycling reactions without further treatment or regeneration. Cu@TiN exhibits good reusability as shown in Figure 8: the reaction conversion maintained 100% for seven cycles while selectivity towards epoxide was 85% in the first reaction run and decreased to 70%. We therefore analyzed Cu@TiN of 4 cycles runs with XPS as shown in Figure S5. Results suggest that CuNPs remain mostly metallic state after one cycle run, the content of CuO in Cu@TiN is increasing with the increase of cycle run number, this is the reason to the epoxidation selectivity dropping. Next, the Cu@TiN photocatalyst was recovered and reactivated in hydrogen gas atmosphere at 200°C for 10 mins, we found the reaction conversion drop to 95% whereas the selectivity towards epoxide regained to 76%. The XPS spectra (Figure S5e) confirmed that the CuNPs are completely reformed to metallic state. In addition, the inductively coupled plasma-atomic emission spectroscopy (ICP-AES) analysis of after-reaction solution indicated only 0.09% of Cu was

leached after one reaction cycle as shown in Table S6. The negligible metal loss is the reason to the good reusability of the novel photocatalyst. Meanwhile, it also demonstrated that the TiN support material not only effectively stabilizes CuNPs in the metallic state but also solidly bonds the NPs avoiding the loss of CuNPs.

Conclusions

In summary, we have developed a stable Cu@TiN photocatalyst for selective epoxidation of alkenes with molecular oxygen as the oxidant. Our characterization and DFT simulations indicate that the stability of metallic state of CuNPs in air is attributed to significant charge transfer between CuNPs and TiN substrate. Photocatalyzed epoxidation processes are driven by visible light irradiation under mild conditions. The novel photocatalyst exhibits with wide substrate scope with various types of alkenes. Interestingly, stereo-selectivity to *trans*-isomer product was observed with stilbene epoxidation. The solvent cyclic ether facilitates the reaction by reacting with molecular oxygen on the surface of CuNPs, yielding oxygen adatoms. This reaction process is driven by light irradiation

at mild temperatures. The reactant alkenes chemically adsorb on CuNPs, forming surface complex. The complex can be activated by irradiation of visible light. The oxygen atoms react with the activated alkene yielding final product of corresponding epoxide. Light irradiation is the driving force of the epoxidation process. Thus, the light intensity and wavelength as well as reaction temperature are influencing parameters on the performance of the photocatalytic epoxidation. The photocatalyst exhibits excellent reusability and an overall reaction pathway for selective epoxidation was proposed. Our results indicate a promising CuNP photocatalyst and photocatalytic methodology at mild reaction conditions for alkene epoxidations by using photocatalysis and molecular oxygen.

ASSOCIATED CONTENT

Supporting Information.

This material is available free of charge via the Internet at <http://pubs.acs.org>.

Calibration curve for conversion determination; Mass spectra for products characterization; Characterization of photocatalyst: XPS, UV-Vis, SEM, EDX; Detailed reaction condition optimization; ICP test for metal loss after reaction.

AUTHOR INFORMATION

Corresponding Author

*E-mail: s.sarina@qut.edu.au; hy.zhu@qut.edu.au

ACKNOWLEDGMENT

Authors gratefully acknowledge financial support from the Australis Research Council. (DP150102110)

KEYWORDS.

Selective epoxidation; Air-stable CuNPs; Photocatalysis; Direct electron photoexcitation; Visible Light; Asymmetric synthesis.

REFERENCES

- Xia, Q. H.; Ge, H. Q.; Ye, C. P.; Liu, Z. M.; Su, K. X. *Chem. Rev.* **2005**, *105*, 1603-1662.
- Studer, A.; Curran, D. P. *Angew. Chem. Int. Ed.* **2016**, *55*, 58-102.
- Keylor, M. H.; Matsuura, B. S.; Stephenson, C. R. J. *Chem. Rev.* **2015**, *115*, 8976-9027.
- Fingerhut, A.; Serdyuk, O. V.; Tsogoeva, S. B. *Green Chem.* **2015**, *17*, 2042-2058.
- rWong, O. A.; Shi, Y. *Chem. Rev.* **2008**, *108*, 3958-3987.
- Wang, C.; Yamamoto, H. *Chem. Asian J.* **2015**, *10*, 2056-2068.
- De Faveri, G.; Ilyashenko, G.; Watkinson, M. *Chem. Soc. Rev.* **2011**, *40*, 1722-1760.
- Deng, X.; Friend, C. M. *J. Am. Chem. Soc.* **2005**, *127*, 17178-17179.
- Cropley, R. L.; Williams, F. J.; Urquhart, A. J.; Vaughan, O. P. H.; Tikhov, M. S.; Lambert, R. M. *J. Am. Chem. Soc.* **2005**, *127*, 6069-6076.
- Linic, S.; Barteau, M. A. *J. Am. Chem. Soc.* **2002**, *124*, 310-317.
- Linic, S.; Barteau, M. A. *J. Am. Chem. Soc.* **2003**, *125*, 4034-4035.
- Williams, F. J.; Bird, D. P. C.; Palermo, A.; Santra, A. K.; Lambert, R. M. *J. Am. Chem. Soc.* **2004**, *126*, 8509-8514.
- Torres, D.; Lopez, N.; Illas, F.; Lambert, R. M. *J. Am. Chem. Soc.* **2005**, *127*, 10774-10775.
- Zhang, N.; Yang, M.-Q.; Liu, S.; Sun, Y.; Xu, Y.-J. *Chem. Rev.* **2015**, *115*, 10307-10377.
- Zhang, Y.; Zhang, N.; Tang, Z.-R.; Xu, Y.-J. *Chem. Sci.* **2012**, *3*, 2812-2822.
- Zhang, Y.; Zhang, N.; Tang, Z.-R.; Xu, Y.-J. *ACS Nano* **2012**, *6*, 9777-9789.
- Weng, B.; Quan, Q.; Xu, Y.-J. *J. Mater. Chem. A* **2016**, *4*, 18366-18377.
- Brus, L. *Acc. Chem. Res.* **2008**, *12*, 41, 1742-1749.
- Smith, J. G.; Faucheaux, J. A.; Jain, P. K. *Nano Today* **2015**, *10*, 67-80.
- Xiao, Q.; Jaatinen, E.; Zhu, H. *Chem. Asian J.* **2014**, *9*, 3046-3064.
- Sarina, S.; Waclawik, E. R.; Zhu, H. *Green Chem.* **2013**, *15*, 1814-1833.
- Zhou, L.; Zhang, C.; McClain, M. J.; Manjavacas, A.; Krauter, C. M.; Tian, S.; Berg, F.; Everitt, H. O.; Carter, E. A.; Nordlander, P.; Halas, N. J. *Nano Lett.* **2016**, *16*, 1478-1484.
- Peiris, S.; McMurtrie, J.; Zhu, H. *Catal. Sci. Tech.* **2016**, *6*, 320-338.
- Chen, X.; Zhu, H. Y.; Zhao, J. C.; Zheng, Z. F.; Gao, X. P. *Angew. Chem. Int. Ed.* **2008**, *47*, 5353-5356.
- Zhu, H. Y.; Ke, X. B.; Yang, X. Z.; Sarina, S.; Liu, H. W. *Angew. Chem. Int. Ed.* **2010**, *49*, 9657-9661.
- Christopher, P.; Xin, H.; Linic, S. *Nat. Chem.* **2011**, *3*, 467-472.
- Zhang, N.; Han, C.; Xu, Y.-J.; Foley Iv, J. J.; Zhang, D.; Cordington, J.; Gray, S. K.; Sun, Y. *Nat. Photon* **2016**, *10*, 473-482.
- Fuku, K.; Hayashi, R.; Takakura, S.; Kamegawa, T.; Mori, K.; Yamashita, H. *Angew. Chem. Int. Ed.* **2013**, *52*, 7446-7450.
- Wen, M.; Kuwahara, Y.; Mori, K.; Yamashita, H. *Top. Catal.* **2016**, *59*, 1765-1771.
- Liu, Z.; Huang, Y.; Xiao, Q.; Zhu, H. *Green Chem.* **2016**, *18*, 817-825.
- Sarina, S.; Zhu, H. Y.; Jaatinen, E.; Xiao, Q.; Liu, H. W.; Jia, J. F.; Chen, C.; Zhao, J. *J. Am. Chem. Soc.* **2013**, *135*, 5793-5801.
- Xiao, Q.; Liu, Z.; Bo, A.; Zavahir, S.; Sarina, S.; Bottle, S.; Riches, J. D.; Zhu, H. *J. Am. Chem. Soc.* **2015**, *137*, 1956-1966.
- Marimuthu, A.; Zhang, J.; Linic, S. *Science* **2013**, *339*, 1590-1593.
- Liu, C.; Yang, B.; Tyo, E.; Seifert, S.; DeBartolo, J.; von Issendorff, B.; Zapol, P.; Vajda, S.; Curtiss, L. A. *J. Am. Chem. Soc.* **2015**, *137*, 8676-8679.
- Guo, X.; Hao, C.; Jin, G.; Zhu, H.-Y.; Guo, X.-Y. *Angew. Chem. Int. Ed.* **2014**, *53*, 1973-1977.
- Jeon, S.-J.; Walsh, P. J. *J. Am. Chem. Soc.* **2003**, *125*, 9544-9545.
- Mizuno, N.; Yamaguchi, K.; Kamata, K. *Coord. Chem. Rev.* **2005**, *249*, 1944-1956.
- Nishiyama, Y.; Nakagawa, Y.; Mizuno, N. *Angew. Chem. Int. Ed.* **2001**, *40*, 3639-3641.
- Schröder, K.; Join, B.; Amali, A. J.; Junge, K.; Ribas, X.; Costas, M.; Beller, M. *Angew. Chem. Int. Ed.* **2011**, *50*, 1425-1429.
- Wei, W.; Zhao, W.; White, J. M. *J. Am. Chem. Soc.* **2004**, *126*, 16340-16341.
- Garcia, M. *J. Phys. D: Appl. Phys.* **2011**, *44*, 283001-283021.
- Yin, M.; Wu, C.-K.; Lou, Y.; Burda, C.; Koberstein, J. T.; Zhu, Y.; O'Brien, S. *J. Am. Chem. Soc.* **2005**, *127*, 9506-9511.
- Yang, L.; He, J.; Zhang, Q.; Wang, Y. *J. Catal.* **2010**, *276*, 76-84.
- Jana, S.; Dutta, B.; Bera, R.; Koner, S. *Langmuir* **2007**, *23*, 2492-2496.

- 1
2
3
4
5
6
7
8
9
10
11
12
13
14
15
16
17
18
19
20
21
22
23
24
25
26
27
28
29
30
31
32
33
34
35
36
37
38
39
40
41
42
43
44
45
46
47
48
49
50
51
52
53
54
55
56
57
58
59
60
- (45) Murphy, A.; Pace, A.; Stack, T. D. P. *Org. Lett.* **2004**, *6*, 3119-3122.
- (46) Dubois, G.; Murphy, A.; Stack, T. D. P. *Org. Lett.* **2003**, *5*, 2469-2472.
- (47) Murphy, A.; Dubois, G.; Stack, T. D. P. *J. Am. Chem. Soc.* **2003**, *125*, 5250-5251.
- (48) Song, Y. J.; Lee, S. H.; Park, H. M.; Kim, S. H.; Goo, H. G.; Eom, G. H.; Lee, J. H.; Lah, M. S.; Kim, Y.; Kim, S.-J.; Lee, J. E.; Lee, H.-I.; Kim, C. *Chem. Eur. J.* **2011**, *17*, 7336-7344.
- (49) Hyun, M. Y.; Kim, S. H.; Song, Y. J.; Lee, H. G.; Jo, Y. D.; Kim, J. H.; Hwang, I. H.; Noh, J. Y.; Kang, J.; Kim, C. *J. Org. Chem.* **2012**, *77*, 7307-7312.
- (50) Hauschild, A.; Karki, K.; Cowie, B. C. C.; Rohlfing, M.; Tautz, F. S.; Sokolowski, M. *Phys. Rev. Lett.* **2005**, *94*, 036106-036109.
- (51) Kovalenko, S. A.; Dobryakov, A. L.; Ioffe, I.; Ernstring, N. P. *Chem. Phys. Lett.* **2010**, *493*, 255-258.
- (52) Lignier, P.; Morfin, F.; Mangematin, S.; Massin, L.; Rousset, J.-L.; Caps, V. *Chem. Commun.* **2007**, *2*, 186-188.
- (53) Hashimoto, K.; Masuda, Y.; Kominami, H. *ACS Catal.* **2013**, *3*, 1349-1355.
- (54) Kale, M. J.; Avanesian, T.; Xin, H.; Yan, J.; Christopher, P. *Nano Lett.* **2014**, *14*, 5405-5412.
- (55) Cheng, Y. H.; Subramaniam, V. P.; Gong, D.; Tang, Y.; Highfield, J.; Pehkonen, S. O.; Pichat, P.; Schreyer, M. K.; Chen, Z. *J. Solid State Chem.* **2012**, *196*, 518-527.
- (56) Sarina, S.; Jaatinen, E. A.; Xiao, Q.; Huang, Y.; Christopher, P.; Zhao, J.; Zhu, H. J. *Phys. Chem. Lett.* **2017**, *8*, 2526-2534.
- (57) Linic, S.; Aslam, U.; Boerigter, C.; Morabito, M. *Nat. Mater.* **2015**, *14*, 567-576.
- (58) Allen, S. E.; Walvoord, R. R.; Padilla-Salinas, R.; Kozlowski, M. C. *Chem. Rev.* **2013**, *113*, 6234-6458.
- (59) Spitzer, A.; Lüth, H. *Surf. Sci.* **1982**, *118*, 121-135.
- (60) Spitzer, A.; Lüth, H. *Surf. Sci.* **1982**, *118*, 136-144.

Entry for the Table of Contents

